

Assessing the Local Isotropy of a Turbulent Plume in Linearly Stratified Saltwater using PIV Data

Wei Zhang^{1,2}, Zhiguo He^{1,3*}, Liang Zhao¹ and Houshuo Jiang²

¹Institute of Coastal and Offshore Engineering
Zhejiang University, Zhoushan 316021, China

²Department of Applied Ocean Physics and Engineering
Woods Hole Oceanographic Institution, Woods Hole 02543, USA

³Second Institute of Oceanography
State Oceanic Administration, Hangzhou 310012, China

Abstract

The local isotropy of turbulent plume flow in linearly stratified saltwater was examined by using the particle image velocimetry (PIV) technique. Linear stratification was produced in a 50×50×50 cm plexiglas tank by using the two-tank method. The plume was created by injecting dense fluid downward near the top of the stratified column. Images of seeding particles in the flow were recorded at 100 Hz. For statistically steady plume flow, instantaneous two-dimensional (2D) velocity vector fields were calculated by using the standard cross-correlation approach. The PIV flow data were then used to calculate local entrainment coefficient, turbulent energy spectra, and local isotropy. It is shown that the mean vertical velocity component fits the Gaussian distribution well. Local entrainment coefficient remains approximately constant (~0.12) until ~0.6Z_{max} but decreases above that height. The Kolmogorov -5/3 spectral slope is evident in the one-dimensional spatial spectra, indicating the existence of the inertial subrange. Values of u_{rms}/w_{rms} in most chosen regions are larger than 0.7, suggesting good local isotropy in the plume turbulence. The present experiments show that buoyant plumes in a linearly stratified environment are isotropic and intensely turbulent even at low velocity.

Themes: Experimental techniques; Oceanography; Turbulence

Introduction

Fluids from hydrothermal vents ascend as turbulent plumes, which transport high concentrations of particulates and heat, mixing and interacting extensively with ambient seawater [1,2]. Mixing and transport in stratified seawater, having significant influence on formation and variation of mineralization and chemical reactions, remain topics of fundamental importance in ocean.

As a nonintrusive measurement method for quantitative flow visualization and to obtain flow structures, particle image velocimetry (PIV) has been developed for over 30 years and applied by researchers to investigate the flow transport and mixing properties, especially in oceanic measurements [3]. PIV is a widely adopted technique and can provide more real solutions compared with numerical simulation which allows detailed prediction [4].

In this paper, we focus on assessing the local isotropy of a turbulent plume in linear stratification using PIV data. The experimental method and apparatus are described briefly in section 2. Section 3 contains the experimental results which are divided into three parts: (i) plume characterization, (ii) spatial energy spectra, (iii) local isotropy assessing.

Experimental Setup and Conditions

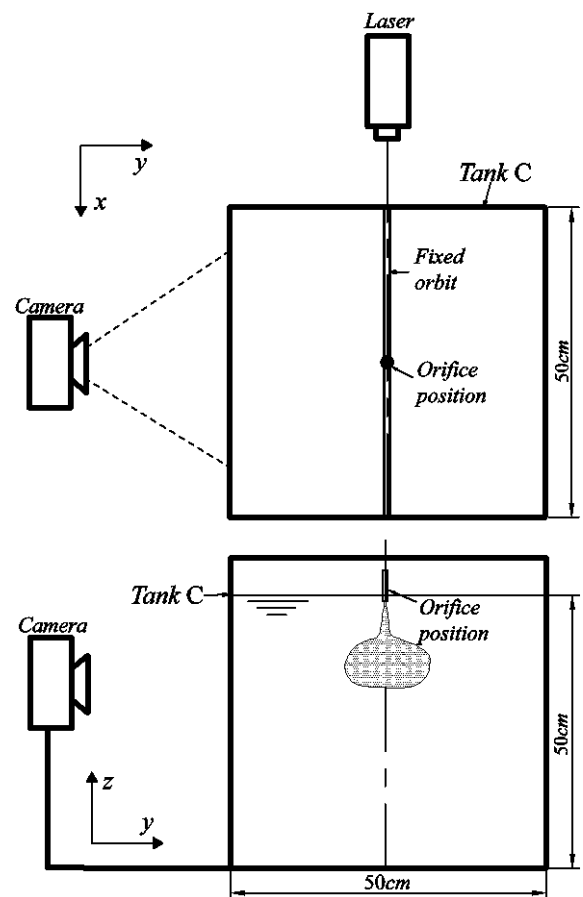


Figure 1. Schematic drawing of the experimental set-up using 2D PIV technique. The upper figure is from top view; the lower figure is from side view.

The experiments were carried out in the Laboratory of Ocean Engineering at Zhejiang University. Side and top views of experimental setup appear in Figure 1. A cubic Plexiglas Tank C with dimension of 50×50×50 cm was filled with linearly stratified saltwater to a depth of 47 cm, using the two-tank method [5]. The copper orifice with diameter of 7 mm was mounted in the center of a fixed orbit which was located on the top of Tank C and the source continuously injecting dense saltwater of density ρ_0 from a reservoir was 3 cm below the saltwater surface. The outflow was controlled by a pump and a flowmeter and therefore maintained steady during an entire experiment. Density on each level was obtained by the equation

of seawater state and the density profile was obtained by linear fitting.

The PIV images were obtained using a CCD camera with the spatial resolution of 2320×1726 pixels in combination with a neodymium-doped yttrium aluminum garnet (Nd:YAG) laser operated at a power of 10W. The camera focused an approximate 25×20 cm x-z 2D plane. 2D velocity vectors are retrieved by cross-correlating two serially measured images at an arbitrarily fixed sampling rate of 100Hz using Davis 8.3, a PIV analysis software, and are calculated from the interrogation window of 32×32 pixels that has 50% overlap with its adjacent ones, corresponding to a spatial resolution of about 1.8 mm [6]. The seeding particles in the present experiments are 15-μm-diameter polyamid spheres, and the density of which is matched to the fluid.

The parameters for all 6 cases are listed in Table 1. According to the scaling of maximum plume penetration in the MTT model, we chose the buoyancy frequency (N), the source density (ρ₀) and the source volume flux (Q) as the controllable variables. The other related parameters in addition are B, the source buoyancy flux; Z_{max}, the measured maximum penetration level of the plume.

According to Jiang and Breier [4], plume development will reach steady state after t*. Here t* is the buoyancy time scale and defined as t*=2π/N where N is the ambient buoyancy frequency. We adopted 3≤t*≤5 from the entire recording time of each case and conducted ensemble average to calculate turbulent properties.

Exp.	N (s ⁻¹)	ρ ₀ (kgm ⁻³)	Q (m ³ s ⁻¹)	B (m ⁴ s ⁻³)	Z _{max} (m)
1	0.66	1005.8	3.24×10 ⁻⁶	2.04×10 ⁻⁷	0.1148
2	0.55	1018.7	3.90×10 ⁻⁶	6.75×10 ⁻⁷	0.1257
3	0.57	1018.7	2.55×10 ⁻⁶	4.60×10 ⁻⁷	0.1138
4	0.66	1026.3	3.06×10 ⁻⁶	8.05×10 ⁻⁷	0.1292
5	0.82	1026.3	3.43×10 ⁻⁶	8.01×10 ⁻⁷	0.1248
6	0.88	1026.3	3.23×10 ⁻⁶	8.17×10 ⁻⁷	0.0988

Table 1. Summary of the experiments.

Experimental Results

Plume Characterization

Figure 2A presents the time-averaged velocity vector of Case 3. It is obviously shown that velocity gets larger from edge to central at the same vertical level in the plume stem and reaches maximum at around the plume centerline. The flow regime above lateral spreading flow shows self-similar and background flow is entrained inwardly at the edge. When the plume develops fully turbulence, vertical velocity profiles fit the Gaussian distribution (Fig. 2B):

$$w_G = w_m e^{-(x-x_m)^2/r^2} \quad (1)$$

where w_m is the centerline vertical velocity located at (x_m, z), and r is radial scale for mean vertical velocity. r evolves linearly and can be fitted to a function of penetration depth z:

$$r = c z + r_0 \quad (2)$$

where linear slope c is the expansion rate of mean vertical velocity and found to be 0.14 in present study, which is in agreement with that in literatures [7]. For plumes, entrainment coefficient α_e can be scaled as:

$$\alpha_e = \frac{5}{6} c \quad (3)$$

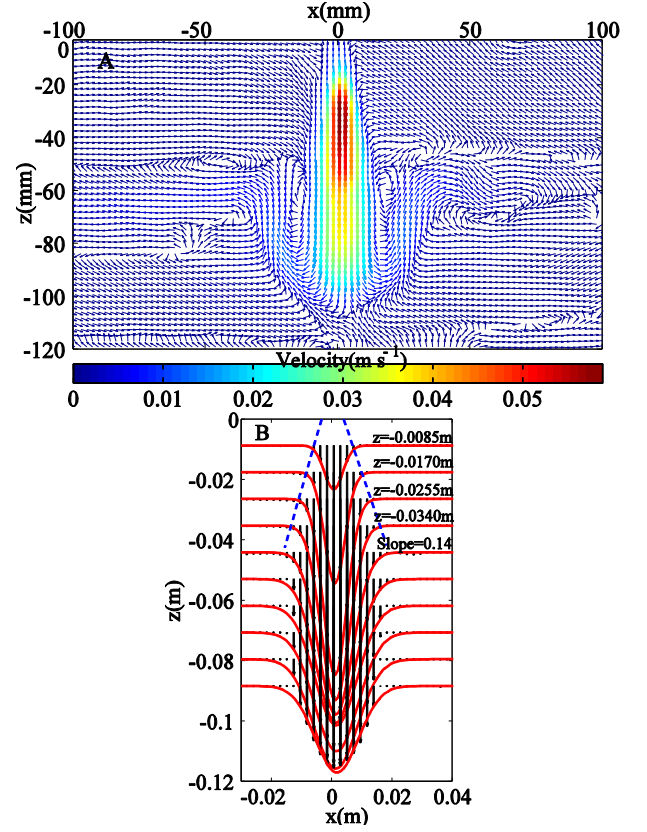


Figure 2. Ensemble averaged velocity vector of Case 3 (A) and its Gaussian fitting to vertical velocity component profile (B). Origin is the location of vent.

Entrainment coefficient distributions along plume penetration normalized by the maximum penetration calculated from Eq. (1) to (3) is shown in Figure 3. In present experiments, the local entrainment coefficient α_e is around 0.12 above ~0.6Z_{max} and becomes negative below ~0.6Z_{max} where the density of plume is equal to that of background after entraining inward saltwater and plume starts to spread laterally (Fig. 2).

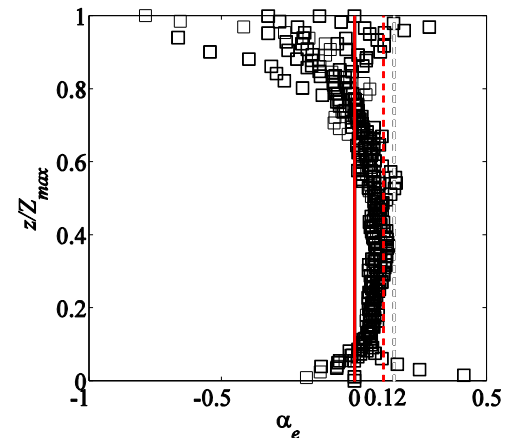


Figure 3. The distribution of entrainment coefficient α_e along plume penetration (z) normalized by the maximum penetration depth (Z_{max}).

Spatial Energy Spectrum

Energy spectra method is a significant way to depict turbulence characteristics. 1D energy spectral density is calculated from:

$$E_{ii}(\kappa_3) = \frac{L}{2\pi n^2} \Sigma F_i(\kappa_3) F_i^*(\kappa_3), \quad (4)$$

where κ_3 is wavenumber in the z-direction, L is the domain length, n is the number of points, F_i means the Fourier transform of velocity component u (when $i=1$) or w (when $i=3$) of the plume centerline and F_i^* indicated the complex conjugate of F_i . Window functions are not required in the Fourier transforms as the PIV data is periodic.

One-dimensional spatial spectra, $E_{11}(\kappa_3)$ and $0.75E_{33}(\kappa_3)$, of the plume centerline are presented in Figure 4. $E_{11}(\kappa_3)$ matching $0.75E_{33}(\kappa_3)$ proves isotropic turbulence spectra. In addition, the collapse of the two curves corresponds to a $-5/3$ slope which means data covers the inertial subrange and extends to dissipation range according to Kolmogorov's second similarity hypothesis [8].

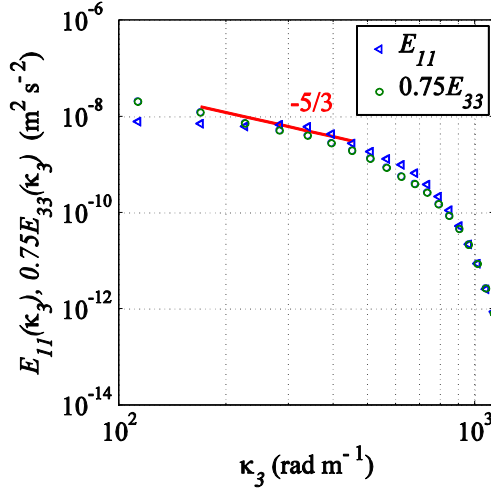


Figure 4. One-dimensional energy spectra, $E_{11}(\kappa_3)$ and $0.75E_{33}(\kappa_3)$, of the plume centerline (Case 3).

Local Isotropy Assessing

In this section, local isotropy will be further tested through velocity statistics calculated from velocity vectors. Webster et al [9] pointed out, for 2D flow field, two sufficient conditions should be met to assess isotropy:

i) the magnitudes of the Reynolds normal stresses are similar, which can be expressed as:

$$\text{urms} \approx \text{wrms} \quad (5)$$

ii) the Reynolds shear stresses and mean velocity are roughly equal to zero as:

$$\begin{aligned} \overline{u'w'} &\approx 0 & \text{and} \\ U &\approx W \approx 0 \end{aligned} \quad (6)$$

where urms and wrms are root-mean square horizontal and vertical velocity respectively, U and W are time-averaged horizontal and vertical velocity respectively.

Ten 5.4mm×12.6mm (3×7 pixels) regions containing outflow (Region 1), plume stem centerline (Region 2), plume cap center (Region 3), maximum penetration (Region 4) and plume edge (Region 5 to 10) were chosen for statistical calculation (Fig. 5). Table 2 summarizes averaged flow statistics calculated from PIV velocity data (\diamond manifests spatially averaged over each region). The characteristics of plume cap center (Region 3) of Case 3 are discussed in particular and compared with other regions which have a similar variation. $\langle \text{urms}/\text{wrms} \rangle$ for most regions above the lateral spreading level is larger than 0.7 except for Region 2 where the maximum velocity appears. And the value for edge region (Region 5 to 8) where entrainment happens is larger than 0.8, which is much close to standard value of 1.0. The region

below the lateral spreading level has a small value of $\langle \text{urms}/\text{wrms} \rangle$, especially on the edge. U and W in the entire flow field are smaller than the order of magnitude 10^{-2} , except for W on the plume centerline. Two criterions for isotropy can be met in other experiments. Thus, most objective regions are homogeneous and isotropic.

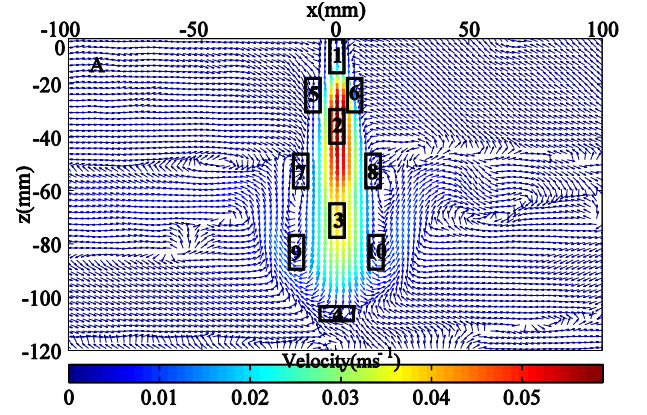


Figure 5. Contour plots of isotropy test in selected regions (Case 3).

Rgn	$\langle U \rangle$ (ms^{-1})	$\langle W \rangle$ (ms^{-1})	$\langle \text{urms}/\text{wrms} \rangle$	$\langle \overline{u'w'} \rangle$ ($\text{m}^2 \text{s}^{-2}$)
1	4.15×10^{-4}	-1.30×10^{-2}	0.7301	7.68×10^{-8}
2	1.80×10^{-3}	-5.00×10^{-2}	0.6661	-1.74×10^{-5}
3	-5.49×10^{-4}	-3.59×10^{-2}	0.8334	5.16×10^{-6}
4	1.82×10^{-5}	5.91×10^{-5}	0.7770	-1.81×10^{-7}
5	6.96×10^{-5}	-4.79×10^{-3}	0.8595	2.28×10^{-6}
6	-8.01×10^{-4}	-6.37×10^{-3}	0.8625	-6.08×10^{-6}
7	9.30×10^{-4}	-4.02×10^{-3}	0.8135	6.88×10^{-6}
8	-1.02×10^{-3}	-8.12×10^{-3}	0.8989	-1.11×10^{-5}
9	-7.02×10^{-3}	3.62×10^{-3}	0.6236	1.39×10^{-5}
10	5.67×10^{-3}	-3.66×10^{-4}	0.6042	-2.22×10^{-5}

Table 2. Summary of statistics for each region.

Conclusions

Local entrainment coefficient remains approximately constant. The Kolmogorov $-5/3$ spectral slope is evident in the one-dimensional spatial spectra. Values of urms/wrms in most chosen regions are larger than 0.7, suggesting good local isotropy in the plume turbulence. The experiments reveal that plume can be isotropic and intensely turbulent in the linear stratification even at low velocity.

Acknowledgments

This work was financially supported by the National Natural Science Foundation of China and Natural Science Foundation of Zhejiang Province under Projects No. 41376095 and LR16E090001 respectively. Wei Zhang was sponsored to study at WHOI by the China Scholarship Council.

References

- [1] Baker E T, Lavelle J W, Massoth G J. Hydrothermal particle plumes over the southern Juan de Fuca Ridge. 1985: 342-344.
- [2] Elderfield H, Schultz A. Mid-ocean ridge hydrothermal fluxes and the chemical composition of the ocean. *Annual Review of Earth and Planetary Sciences*, 1996, 24: 191-224.

- [3] Seol D G, Bhaumik T, Bergmann C, et al. Particle image velocimetry measurements of the mean flow characteristics in a bubble plume. *Journal of engineering mechanics*, 2007, 133(6): 665-676.
- [4] Jiang H, Breier J A. Physical controls on mixing and transport within rising submarine hydrothermal plumes: A numerical simulation study. *Deep Sea Research Part I: Oceanographic Research Papers*, 2014, 92: 41-55.
- [5] Ghajar A J, Bang K. Experimental and analytical studies of different methods for producing stratified flows. *Energy*, 1993, 18(4): 323-334.
- [6] Xi H D, Lam S, Xia K Q. From laminar plumes to organized flows: the onset of large-scale circulation in turbulent thermal convection. *Journal of Fluid Mechanics*, 2004, 503: 47-56.
- [7] Shabbir A, George W K. Experiments on a round turbulent buoyant plume. *Journal of Fluid Mechanics*, 1994, 275: 1-32.
- [8] Pope S B. *Turbulent flows*, Cambridge University Press, 2000.
- [9] Webster D R, Brathwaite A, Yen J. A novel laboratory apparatus for simulating isotropic oceanic turbulence at low Reynolds number. *Limnology and Oceanography: Methods*, 2004, 2(1): 1-12.